Iranian Journal of Chemistry and Chemical Engineering (IJCCE)

Analysis of ionic liquid pretreated low-rank coal *via* equilibrium-based gasification model

Saad Saeed[a*], Sana Saeed[a], Muzaffar Riaz[a]

[a]*Department of Chemical Engineering, NFC Institute of Engineering & Technology, Multan, Pakistan*

[*]*Correspondence concerning this article should be addressed to:*

Engr. Dr. Saad Saeed Email: saadsaeed@nfciet.edu.pk Telephone: +092-331-7135425

ABSTRACT

The utilization of vast coal deposits around the globe as an energy source is significantly limited in scope owing to environmental risks. In this context, ionic liquids (ILs) provide a novel solution as eco-friendly pretreatment agents. This work examined the effects of IL pretreatment on the gasification of low-grade coal using a simulation model in Aspen Plus®. Four ILs, 1-butyl-3-methylimidazolium chloride [Bmim][Cl], 1-ethyl-3-methylimidazolium chloride [Emim][Cl], trihexyltetradecylphosphonium chloride [P_{66614}] [Cl], and tributylmethylammonium chloride [N_{1444}] [Cl], were employed in this study. A comparative and sensitivity analysis was conducted on untreated and IL-pretreated coal samples using an equilibrium-based steam-O_2 gasification model designed in Aspen Plus®. The model was validated and utilized to vary the oxygen/fuel (O_2/F) ratio, steam/fuel (S/F) ratio, and temperature within the specified ranges (700-950°C, 0.1-0.6, and 2-4, respectively). The results showed that all the ILs increased CO and H_2, and decreased CO_2 and CH_4, in the syngas produced by coal gasification. The biggest change was affected by [P_{66614}] [Cl], which increased CO and H_2 from 12 mol% and 42 mol % to 16 mol% and 50 mol %, respectively, and reduced CO_2 and CH_4 from 35 mol% and 3.5 mol% to 29 mol% and 2 mol%, respectively. The lower heating value (LHV) of syngas was increased from 7.37 MJ/Nm^3 for untreated coal to 7.61, 7.56, 8.1, and 7.56 MJ/Nm^3 for coal treated by [Bmim][Cl], [Emim][Cl], [P_{66614}] [Cl], and [N_{1444}] [Cl], respectively. As opposed to raw coal, [Bmim][Cl] and [P_{66614}][Cl] generated more CGE, ENE, and EXE. The highest CGE, ENE, and EXE of 19, 13.3, and 38.3% were achieved by [P_{66614}] [Cl] treated coal. Syngas having higher H_2/CO ratio and LHV were produced at low temperatures, low O_2/F ratio, and high S/F ratio. The results of this investigation demonstrated that ILs composed of ammonium and phosphonium might be useful coal pretreatment agents in thermochemical conversion processes.

KEYWORDS

Low-rank coal; ionic liquids; pretreatment; equilibrium model; Aspen Plus; sensitivity analysis.

1. INTRODUCTION

Pakistan is a nation rich in coal resources, ranked 20th globally, with over 3.377 billion tonnes of confirmed coal reserves [1]. Due to the present energy crisis, coal is attracting the attention of the Government as an energy resource, which can reduce the heavy dependence on imported oil and, consequently, the current account deficit. Several coal-based energy projects under the framework of the China Pakistan Economic Corridor (CPEC) have been recently established. As the government strives to make use of domestic resources, coal's role in the energy industry is expected to expand significantly over the next decade. Pakistan coal predominantly has a high amount of ash, sulfur, and low heating value. Thermochemical conversion of indigenous coal has been subjected to considerable research in recent times [2]–[4]. A major concern is that the syngas obtained by gasifying low-rank lignite coal are likely to contain undesirable amounts of acid gases, i.e., H_2S and CO_2. Lignite contains prominent hydrogen-bonded crosslinks that form futile CO_2 and water, thereby limiting its effective utilization in thermo-chemical conversion processes. Therefore, pretreatment of feed or post-treatment of syngas must be employed to improve the viability of lignite as an energy resource [5].

Pretreatment of coal has proven effective in destroying weak hydrogen bonds, upgrading from low-rank to high-rank, and increasing the heating value [6]. Strict environmental regulations have meant that the traditional pretreatment method of employing acids or alkalis is not feasible anymore. In this respect, ILs have shown to be viable options.

ILs are low-melting salts comprised of an organic cation associated with an anion [7]. They are extensively investigated in diverse scientific applications with promising results [8], [9]. The pioneering work by Painter et al. [10] on the interactions between coal and ILs paved the way for using ILs as pretreatment agents for coal. They argued that imidazolium-based ILs can fragment and disintegrate coal into extremely fine particles, in addition, to releasing the trapped lower molecular weight volatiles. Peng et al. showed that IL pretreatment can destroy crosslinks binding structure with a significant change in the pyrolysis product composition [11]. Pretreatment of lignite by [Bmim][$MeSO_4$] resulted in high breakage of bonds evidenced by a higher rate of decomposition and lower activation energy [12]. In recent times, the use of ILs as pretreatment agents has extended to thermo-chemical conversion processes for both coal and biomass [13]. A significant improvement in the pyrolysis product yield was observed after pretreatment of lignite by [Bmim][Cl][14]. Structural changes and alterations in the thermal profile of sub-bituminous coals under the pretreatment of various imidazolium-based ILs have also been studied [15]. Bai et al. [16] recently discovered that imidazolium-based ILs increased the thermal stability and activation energy of bituminous coal. Yoon et al. [17] used [Bmim][Cl] to pretreat coal, and compared the syngas composition of untreated and IL pretreated coal at various temperatures. It was found that the IL pretreated coal generated less CO_2 and more CO. Moreover, IL pretreated coal was able to produce 1.63 times more H_2 than untreated coal. Optimization of parameters for IL-pretreated low-grade coal is necessary to take the process further [18]. Our recent work [19], in which

ammonium and phosphonium cations, in addition to imidazolium, were used, demonstrated that the ammonium and phosphonium-based ILs could also be promising pretreatment agents for low-rank coal.

Aspen Plus® is a user-friendly, robust, and efficient simulation application for a wide range of pilot-scale and commercial-scale processes [20]. By employing Aspen Plus® modeling and simulation capabilities, designers can potentially attain a comprehensive comprehension of the behavior of the forecasting process [21]. Aspen Plus® has been extensively used in simulating various chemical industrial processes [22]. Predicting the gasification behavior of fuels using kinetic models is difficult, data-intensive, and imprecise. Conversely, equilibrium models based on thermodynamics are more applicable since a responding phase is most stable at equilibrium, exhibiting maximum entropy and minimal Gibbs free energy. In the process sector, thermodynamic equilibrium models are therefore commonly implemented.

This work is an extension of our earlier research, which compared the thermal degradation performance of [Bmim][Cl], [Emim][Cl], [P_{66614}] [Cl], and [N_{1444}] [Cl] for low-rank coal, and evaluated the kinetic and thermodynamic parameters [19]. This study seeks to forecast and examine the gasification efficiency of coal after pretreatment by the four aforementioned ionic liquids using an equilibrium-based gasification model created in Aspen Plus®. This is the first effort, as far as the authors are aware, to model and simulate thermochemical transformation of low-grade coal pretreated with IL. The investigation may facilitate the application of ILs as pretreatment agents to enhance the thermochemical conversion efficiency of low-grade coal.

2. EXPERIMENTAL SECTION

2.1. IL pretreatment and characterization

This study utilized Duki coal sourced from the Baluchistan area of Pakistan. The raw substance was crushed, sieved, ground, and dried. Two imidazolium-based, one ammonium-based, and one phosphonium-based ILs have been employed in the research. The selection of ILs was largely determined by their economic feasibility and accessibility. The pretreatment procedure and the methods employed for the characterization of the samples are already given in our previous work. Untreated coal will be denoted as RC, whereas coal treated with [Bmim][Cl], [Emim][Cl], [P_{66614}] [Cl], and [N_{1444}] [Cl] will be denoted as RC_1, RC_2, RC_3, and RC_4, respectively.

2.2. Aspen Plus® simulation model

Gasification of low-grade coal was simulated using a steady-state equilibrium model as shown in

2.2.1. Model Assumptions

Model assumptions are as follows [23]:

- Coal drying and pyrolysis take place instantaneously at the top of the gasifier.
- Char combustion and gasification occur instantaneously in the gasifier.
- Steady-state, isothermal, and kinetic-free gasification takes place.
- Volatile products mainly contain CO, H_2, CH_4,, CO_2, and H_2O.
- All tar will be considered as C_6H_6.
- Reactions reach equilibrium in the gasifier.
- Gasifier has negligible pressure drop.
- Particle size is not a factor in the calculation.

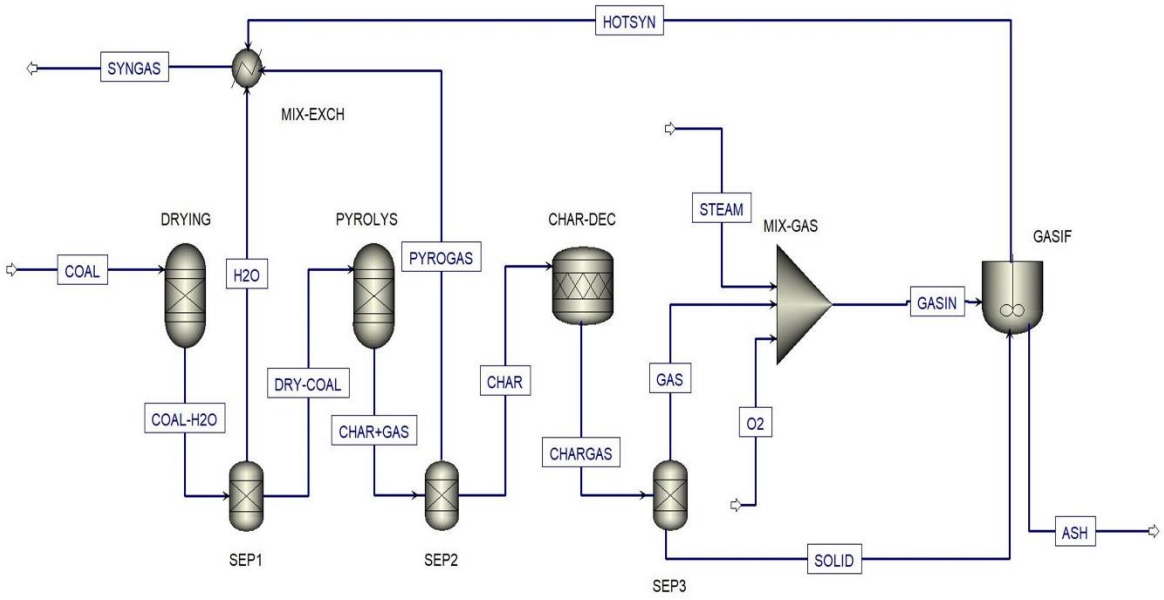

Figure 1: Simulation model for coal gasification in Aspen Plus

2.2.2. Model description

The physical property technique utilized in the model was RK-SOAVE, which is favored in gas processing facilities because of its capability of processing hydrocarbons and light gases (e.g., CO_2 and H_2), as well as its exceptional suitability for places characterized by high temperature and pressure. The stream class chosen is MIXCINC due to the presence of non-conventional components and solids. The enthalpy of coal was calculated using the HCOALGEN model, whereas the density of coal was determined using the DCOALIGT model. Aspen Plus® models are briefly discussed in **Table 1**. The process consisted of three separate phases linked by separators and mixers: drying, pyrolysis, and char gasification and combustion.

Table 1: Process blocks description used in the simulation

Block	Aspen Plus® model	***Description***
DRYING	*RYield*	*Simulates coal drying based on moisture content in coal*
SEP1	*Sep*	*Separates coal from water*
PYROLYS	*RYield*	*Simulates coal pyrolysis*
SEP2	*Sep*	*Separates char from pyrolysis gas*
CHAR-DEC	*RStoic*	*Breaks down char into its fundamental constituents and ash*
SEP3	*Sep*	*Extracts char gas from unconverted char*
GASIFIER	*RGIBBS*	*Simulates char gasification and combustion*
MIX-GAS	*Mixer*	*Mixes steam, O_2, and fuel*
MX-EXCH	*Heater*	*Mixes the product gas and provides heat for coal drying and pyrolysis*

2.2.2.1 *Drying section*

The component properties of coal utilized for model validation in this study were sourced from the research conducted by Wen et al. [24]. The coal first goes through the drying portion, which is replicated by the RYield block in Aspen Plus®. This step focuses only on product yield and does not include stoichiometry or reaction kinetics. Yield w.r.t mass of gaseous water was determined based on the moisture content of coal, assuming that all physically bound water is eliminated throughout the process.

After drying, separator (Sep1 block) separated the gaseous water from coal. Water went to the heat exchanger while dry-coal, to the pyrolysis section.

2.2.2.2 *Pyrolysis section*

Coal pyrolysis was modeled using RYield block since reaction kinetics are unknown and the product yield has been predicted from calculations. Suuberg et al. [25] performed several experiments on the pyrolysis of lignite coal and found a relation between the elemental composition of coal and the pyrolysis product composition. The amount of char was predicted based on the experimental results of Suuberg et al. [25]. The yield of gaseous products was specified based on the correlations developed by Okumura et al. [26]. Pyrolysis section was followed by a separator (Sep2), which separated the gaseous products from the char. The gaseous products go to the heat exchanger, while char goes to char decomposer.

Given the elemental makeup of char, the RStoic block in Aspen Plus® was utilized to mimic char breakdown. In this block, char was broken down into the elements C, O_2, H_2, N_2, S, and ash according to the ultimate analysis. The coefficients were calculated by using Fortran coding in the calculator block. Char decomposer was followed by a separator which separated solids and gaseous products.

2.2.2.3 *Char gasification & combustion section*

RGibbs reactor was used to model gasification. RGibbs reactor works for multiphase chemical equilibrium by minimizing Gibbs free energy. Common gasification reactions are shown in **Table 2**.

The RGibbs model computes the syngas composition by assuming that chemical equilibrium is reached. Ash was separated from the product via separator. The complete set of operating parameters in the gasification model is listed in **Table 3**.

Table 2: Gasification reactions included in the simulation

Reaction #	***Reaction***	***Reaction Name***
01	$C + O_2 \rightarrow CO_2$	*Carbon Combustion reaction*
02	$C + H_2O \rightarrow CO + H_2$	*Water-Gas shift reaction*
03	$C + CO_2 \rightarrow 2CO$	*Boudouard reaction*
04	$C + 2H_2 \rightarrow CH_4$	*Methanation reaction*
05	$CO + H_2O \rightarrow CO_2 + H_2$	*CO shift reaction*
06	$H_2 + 0.5O_2 \rightarrow H_2O$	*Hydrogen combustion reaction*

Table 3: Operating parameters in the simulation model

Feed	*Flow rate (kg/sec)*	*5.44*
	Temperature (°C)	*25*
	Pressure (Pa)	*3.55e+06*
Drying	*Temperature (°C)*	*327*
	Pressure (Pa)	*3.55e+06*
Pyrolysis	*Temperature (°C)*	*627*
	Pressure (Pa)	*3.55e+06*
Char decomposition	*Duty (Watt)*	*0*
	Pressure (Pa)	*3.55e+06*
O₂	*Flow rate (kg/sec)*	*3.27*
	Temperature (°C)	*371*
	Pressure (Pa)	*3.55e+06*
Steam	*Flow rate (kg/sec)*	*15.51*
	Temperature (°C)	*371*
	Pressure (Pa)	*3.55e+06*
Gasifier	*Temperature (°C)*	*900*
	Pressure (Pa)	*3.55e+06*
Heat exchangers	*Pressure (Pa)*	*3.55e+06*

2.2.3. Model Validation

The model was verified by comparing the anticipated syngas composition with the experimental data of Wen et al. [24]. Statistical analysis was performed using Root-mean-square (RMS) and root-sum-squared (RSS) methods which are given as follows [27]:

$$\boldsymbol{RMS} = \sqrt{\frac{\sum_i^N (\boldsymbol{Experiment_i} - \boldsymbol{Model_i})^2}{\boldsymbol{N}}} \qquad (1)$$

Where

N = data points

$$RSS = \sum_{i=1}^{N} \left(\frac{y_{ie} - y_{is}}{y_{ie}}\right)^2 \quad (2)$$

Where

y_{ie} = experimental mole fraction of component i

y_{is} = predicted mole fraction of component i

$$MRSS = \frac{RSS}{N} \quad (3)$$

Where

MRSS = mean-root-sum-squared

$$Mean\ error\ (ME) = \sqrt{MRSS} \quad (4)$$

Table 4 presents a comparison between simulated findings and experimental values. Minor discrepancies in the outcomes might be attributed to the existence of tar, a factor that was not considered in the simulation model. The statistics indicate that the model closely aligns with the experimental data, with a mean error of 0.056. It can accurately forecast syngas composition.

Table 4: Model validation with experimental results

Source	***Product gas composition on a dry basis (mol.%)***				***RMS***	***RSS***	***MRSS***	***Mean Error***
	CO	***CO_2***	***H_2***	***CH_4***				
Experimental work	*27.16*	*22.84*	*38.12*	*9.34*	*0.81*	*0.013*	*0.0032*	*0.056*
Simulation	*26.89*	*22.57*	*39.33*	*8.34*				

2.3. Conversion efficiency

There are various ways to quantitatively define the conversion efficiency of coal to syngas, including cold gas efficiency (CGE), energy efficiency (ENE), and exergy efficiency (EXE).

2.3.1. Cold Gas Efficiency (CGE)

CGE assesses gasification performance and can be determined as follows [28]:

$$\eta_{CGE} = \frac{m_s \times HHV_s}{m_f \times LHV_f} \quad (5)$$

Where ms and mf represent the mass flow rates of syngas and fuel, while HHVs and LHVf refer to the higher heating value and lower heating value of syngas and fuel, respectively.

2.3.2. Energy efficiency (ENE)

Energy efficiency can be easily calculated by applying energy balance to the gasification process, which leads to the following equation [29]:

$$\eta_{ENE} = \frac{\textbf{Energy content in the syngas}}{\textbf{Energy content in fuel} + \textbf{Energy content in steam}} \quad (6)$$

2.3.3. Exergy efficiency (EXE)

EXE can be most aptly defined as [29]:

$$\eta_{EXE} = \frac{\textbf{Exergy of the syngas}}{\textbf{Exergy of fuel} + \textbf{Exergy of steam}} \quad (7)$$

Exergy of fuel can be calculated as follows [29]:

$$\textbf{Exergy of fuel} = \beta \times LHV_f \quad (8)$$

Where β depends on O/C and H/C molar ratios in the fuel and is given as follows:

When O/C ≤ 0.5:

$$\beta = 1.0438 + (0.0158 \times \frac{H}{C}) + (0.0813 \times \frac{O}{C}) \quad (9)$$

When 0.5 < O/C ≤ 2:

$$\beta = \frac{1.0414 + (0.0177 \times \frac{H}{C}) - (0.3328 \times \frac{O}{C}) \times (1 + (0.0537 \times \frac{H}{C}))}{0.4021 \times \frac{O}{C}} \quad (10)$$

LHV_f can be obtained from HHV of fuel:

$$LHV_f = 0.943 \times HHV_f \quad (11)$$

Exergy of syngas can be calculated by the following equation:

$$\textbf{Exergy}_{syngas} = \sum_i X_i \, Ex_{o,i} + RT_0 \sum_i X_i ln X_i \quad (12)$$

Where X_i is the mole fraction and $Ex_{o,i}$ is the standard chemical exergy of component i in the syngas. The Ex_o of CO, CO_2, H_2, and CH_4 are 275100, 19870, 236100, and 831650 kJ/kmol, respectively [29].

3. RESULTS AND DISCUSSION

3.1. Comparative analysis at standard model conditions

Untreated and IL-treated coal samples were gasified using the equilibrium model developed in Aspen Plus®. Syngas composition in terms of mole fractions obtained at standard model parameters, T=900°C, O_2/fuel ratio=0.6, and steam/fuel (S/F) ratio=2.85, for the different samples, are plotted in **Figure 2.** The higher temperature was chosen for IL reactivity comparison as it has been reported that gasification of IL-pretreated fuel shows lower activity initially, possibly due to reactive components and minerals washed away by distilled water during pretreatment. IL pretreatment decreases the ash content in coal, reducing fouling and slagging in gasification equipment, but also diminishing the ash's catalytic properties during gasification. Nevertheless, the decrease is balanced out by the rise in C=O bonds as a result of IL pretreatment. The CO concentration of the samples varied from 0.12-0.16, with untreated coal showing the lowest value. Since the temperature is high (900°C), a higher concentration of CO is obtained as expected due to the dominance of the Boudouard reaction [28]. All ILs increased CO concentration, which is similar to the findings of Yoon et al. [17] in a research where coal underwent pretreatment with [Bmim][Cl] followed by steam gasification in a fixed bed reactor. BET analysis on coal pretreated by [Bmim][Cl] showed that at high temperatures, gas diffusion into pores becomes the rate-controlling step. Due to pretreatment, the size of the pores increased tremendously, with many micropores converted into mesopores. CO concentration was found to be directly proportional to the sum of carbon and oxygen in each sample.

Regarding CO_2, untreated coal recorded the highest value, whereas [P_{66614}] [Cl] gave the lowest value. Almost same values were calculated for [Bmim][Cl], [Emim][Cl], and [N_{1444}] [Cl]. [P_{66614}] [Cl] treated coal contains much less O_2 as compared with other samples. This could be the main reason for the low CO_2 concentration. This result is environmentally beneficial since CO_2 is the main contributor to global warming, and techniques are being developed to reduce its emissions, especially from plants using fossil fuels like coal. High CO_2 concentrations are also one of the main deterrents to using low-rank coal at the commercial level for energy production purposes. [N_{1444}] [Cl] also showed slightly less CO_2 content than raw coal, which may be again due to less O_2 in the sample. Yoon et al. [17] observed that at 900°C, [Bmim][Cl] increased the CO_2 content of Indonesian low-rank coal. However, the elemental composition of Indonesian low-rank coal differed very much from the coal used in this study (H/C and O/C being 0.054 and 0.268, and 0.091 and 0.233 for Indonesian low-rank coal and the coal used in this study, respectively). This suggests that the elemental composition of the subject coal has a significant bearing on the behavior of IL treatment.

Water-gas-shift (WGS) reaction is mainly responsible for producing H_2, as shown in **Table 2**. In the WGS reaction, carbon combines with steam to form water gas, a combination of CO and H_2. [P_{66614}] [Cl] upgrades the low-rank coal, increasing the carbon content from 57.77 to 82.75%, which equals a 43% increase. This leads to an H_2-rich syngas, confirmed by the results. The other three ILs also

increased the H_2 concentration, owing to a higher carbon content than untreated coal. The H_2 concentration results for [Bmim][Cl] are in agreement with those reported by Yoon et al. [17], in which H_2 also increased for IL-pretreated coal.

A low concentration of CH_4 was obtained since the methanation reaction favors low temperatures. Comparatively, all IL-treated samples lowered CH_4 concentration by a wide margin, e.g., [P_{66614}] [Cl] reduced CH_4 from 0.035 to 0.019. An important and useful parameter to measure the quality of syngas is the H_2/CO ratio [30]. H_2/CO ratios for the samples ranged from 3.13-3.53. The highest H_2/CO ratio was obtained for the untreated coal due to very low CO concentration, which offset the low concentration of H_2 content.

LHV is the function of CO, H_2, and CH_4 in the syngas, and was calculated from the following correlation [31]:

$$\boldsymbol{LHV_{syngas} = 0.0042 \times (30 \times CO + 25.7 \times H_2 + 85.4 \times CH_4)} \quad \textit{(13)}$$

LHV of the IL-treated samples exhibited higher values than untreated coal and followed the order; RC_3>RC_1>RC_4>RC_2>RC. The values were in the range of 7.38-8.1 MJ/Nm^3. In raw coal, the low concentrations of CO and H_2 in syngas balance the high concentration of CH_4, resulting in relatively lower LHV.

Figure 3 shows the CGE, ENE, and EXE of the samples at standard model conditions. The acquired CGE values were in proximity, with [P_{66614}] [Cl] slightly ahead. This result could be explained based on the higher LHV of the syngas produced by [P_{66614}] [Cl] treated sample since the LHV of the fuels did not show much difference. A similar trend was observed for ENE, albeit having much smaller values than CGE, around 0.12, as compared to 0.18 for CGE. The order of CGE and ENE was decided by the ratio of LHV of syngas and LHV of the fuel. However, higher values above 0.30 were obtained for EXE, with [P_{66614}] [Cl] treated coal again, giving the highest value. This is due to higher syngas exergy for [P_{66614}] [Cl] treated coal, affected by syngas composition. This agrees with the exergy analysis studies done on [Bmim][Cl] pretreated coal by Yoon et al. [17] previously in which it was found that IL-pretreated coal shows higher EXE as compared to untreated coal.

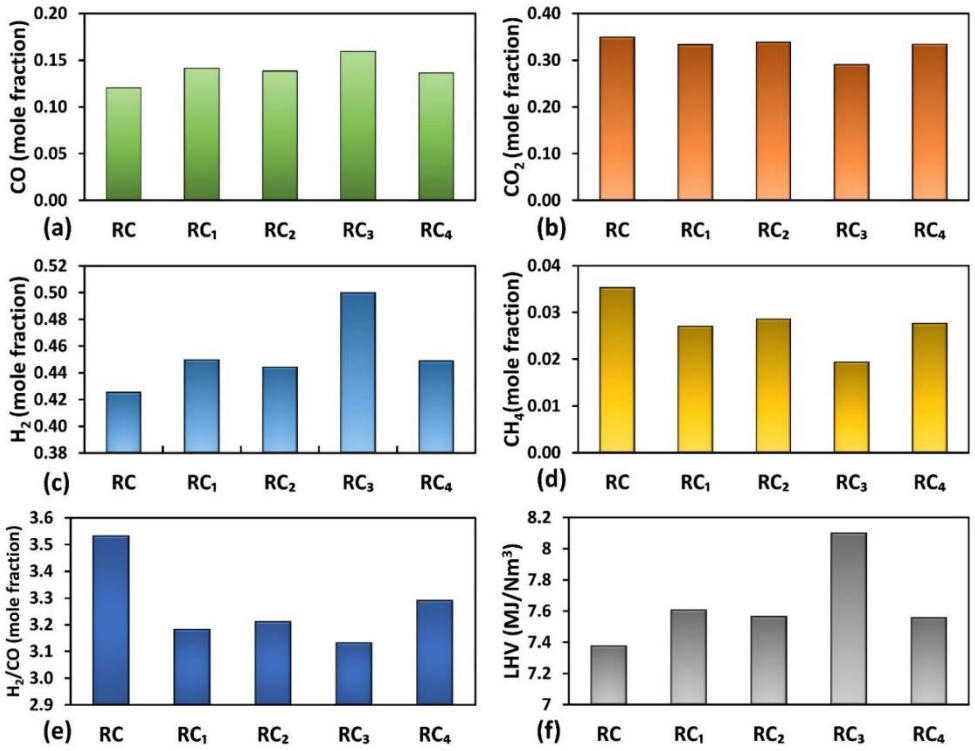

Figure 2: Syngas composition at standard model conditions of T = 900°C, O_2/F = 0.6, S/F = 2.85 (a) CO (b) CO_2 (c) H_2 (d) CH_4 (e) H_2/CO (f) LHV

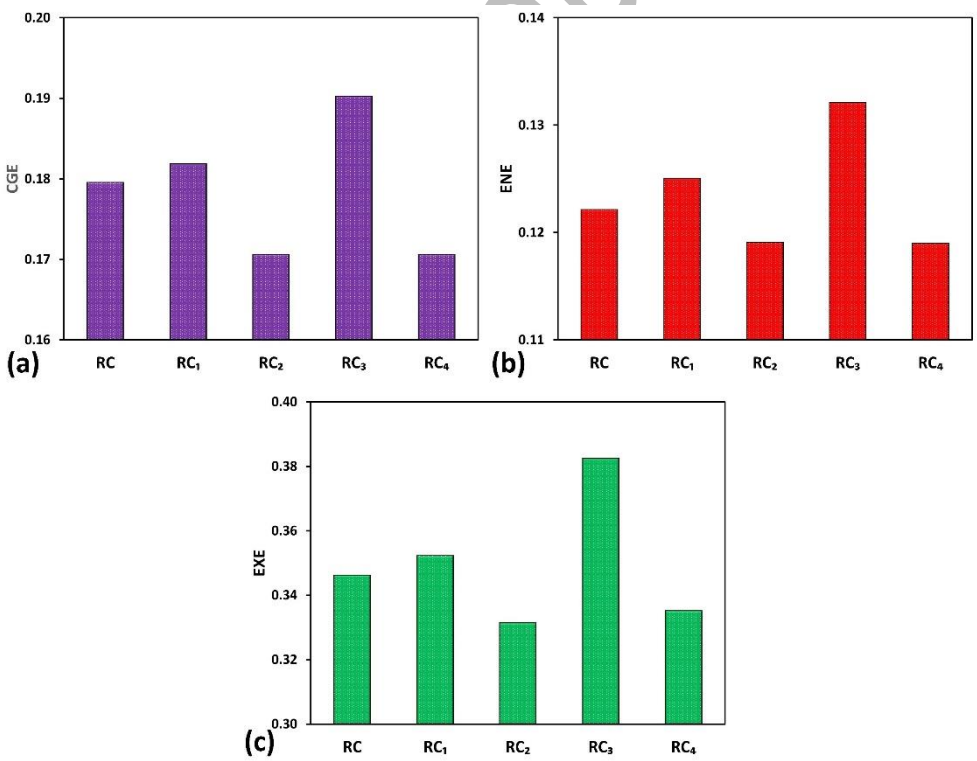

Figure 3: (a) CGE (b) ENE (c) EXE of untreated and IL-treated coal samples

3.2. Effect of temperature

Figure 4 displays the impact of temperature on syngas composition for both untreated and IL-treated coal samples. At low temperatures, both carbon and methane remain unburnt in the fuel, and carbon conversion is very low [28]. As the temperature increases, more carbon gets converted into CO due to the Boudouard reaction. Moreover, CH_4 is also converted into H_2 by the reverse methanation reaction, resulting in higher H_2 and CO concentrations and improving the LHV of the syngas. Therefore, the temperature was varied from 700 to 950°C keeping O_2/F and S/F constant at 0.6 and 2.85, respectively. With the increase in temperature, CO increased, and CO_2 decreased for all the samples. This is in accordance with the Boudouard reaction, which implies that higher temperature favors the production of CO at the expense of CO_2. Sharper slopes were observed for IL-treated samples than untreated coal, especially in the case of [P_{66614}] [Cl] treated coal. Among the ILs, [P_{66614}] [Cl] showed the highest fluctuation with CO increasing from 0.07 at 700°C to 0.17 at 950°C.

Yoon et al. [17] demonstrated that pretreated coal takes more time to convert than untreated coal, possibly due to the transfer of reactive functional groups to ILs during pretreatment, which is subsequently washed away by distilled water. The results of this study concur with these findings. However, this reasoning does not explain the significant rise in CO for [P_{66614}] [Cl] treated coal since [P_{66614}] [Cl] was fully absorbed by coal and did not require any washing. It was shown in our previous study that [P_{66614}] [Cl] treatment increases carbon and decreases the O_2 of coal to a large extent [32]. Thus, it could be implied that [P_{66614}] [Cl] treatment upgrades the coal, which makes it behave differently. The highest CO and lowest CO_2 concentrations at increasing temperatures (above 900°C) were calculated for [P_{66614}] [Cl] treated coal. It has been shown previously that H_2 content increases sharply at low temperatures and then decreases slowly with the temperature rise [33].

A similar pattern was observed for all the samples in this study, with 850°C being the point of inflection. Regarding H_2, there was a linear decrease for the samples, except RC_3, which exhibited an exponential decrease in the temperature range of 700-800°C. This is attributed to the dominance of the WGS reaction at the start before the combustion reaction takes over. The production of CH_4 is caused by the methanation reaction, which is exothermic and favors low temperatures. Due to the higher carbon and H_2 content, [P_{66614}] [Cl] showed higher CH_4 content in the beginning but decreased sharply at higher temperatures, eventually reaching the minimum value of 0.017 at 950°C. This might be attributed to the regulating influence of the Boudouard and WGS reactions.

As temperature increases, CO increases, and H_2 decreases. Therefore, the H_2/CO ratio decreased with the temperature rise. The decrease was more pronounced in the case of [P_{66614}] [Cl] treated coal, which gave the highest values among the studied samples at 700 and 750°C. [N_{1444}] [Cl] yielded greater H_2/CO ratios compared to imidazolium-based ILs overall. In terms of LHV, a large disparity was observed with [P_{66614}] [Cl] treated coal recording higher values than other samples. This is due to higher H_2 and CO

content in [P_{66614}] [Cl] treated coal. All ILs gave higher values than untreated coal, which shows that IL pretreatment results in making coal more efficient with reduced CO_2 and CH_4 content.

Figure 5 illustrates the effect of temperature on CGE, ENE, and EXE. Similar trends were observed for CGE and ENE, with both showing a linear rise for each sample. LHV of the syngas and the fuel played a key role in shaping the curves of CGE and ENE. As a result, the same order was observed for both efficiencies. [P_{66614}] [Cl] treated coal gave the highest values, followed by [Bmim] [Cl], while other samples did not show much difference. This is due to the higher HHV of syngas produced by [P_{66614}] [Cl] and [Bmim] [Cl]. EXE followed the same order, i.e. RC_3> RC_1>RC>RC_4> RC_2. The exergy of syngas was the main factor behind this order of EXE, which depends on the syngas composition. The higher concentration of H_2 in the syngas increased its exergy, which ultimately resulted in greater EXE.

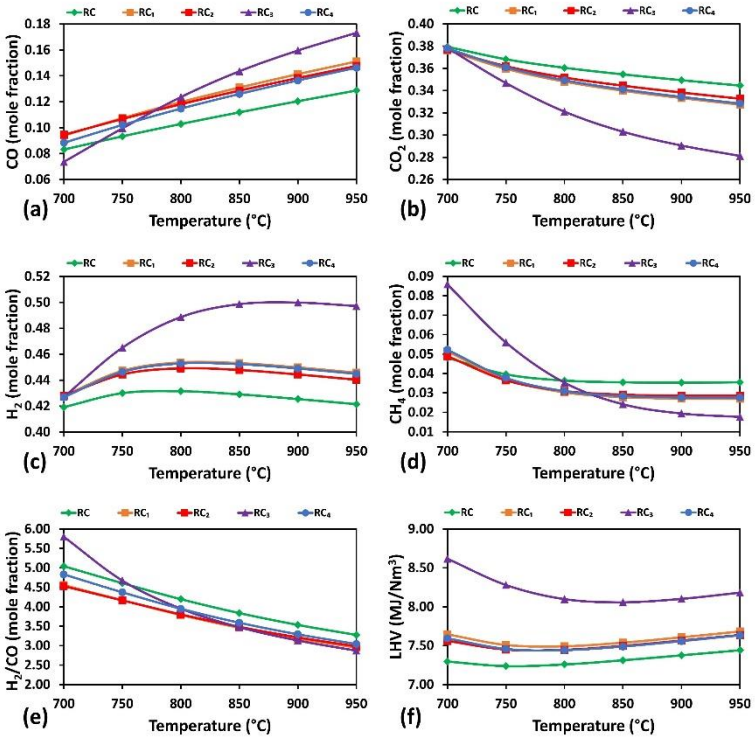

Figure 4: Effect of temperature at O_2/F=0.6 and S/F=2.85 on syngas composition (a) CO (b) CO_2 (c) H_2 (d) CH_4 (e) H_2/CO (f) LHV

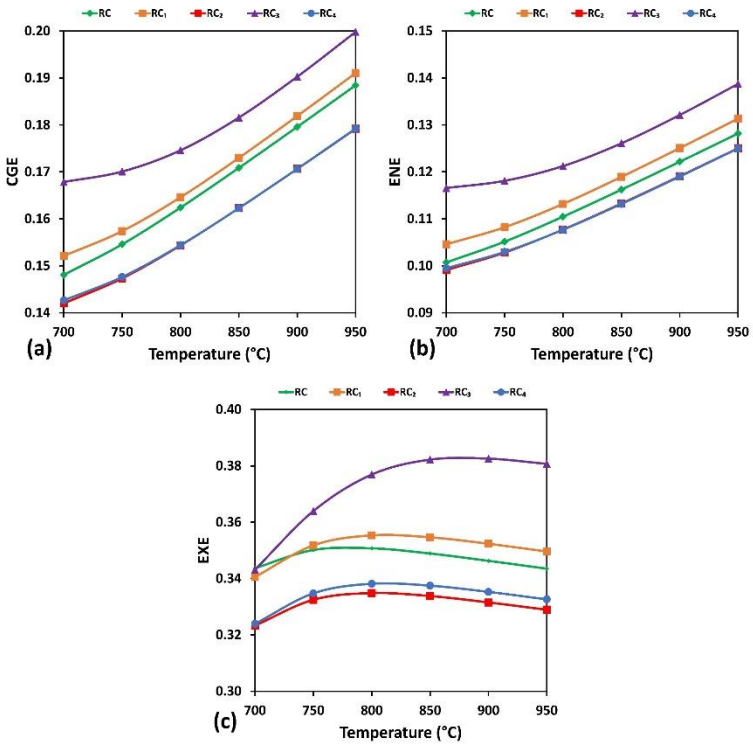

Figure 5: Effect of temperature on (a) CGE (b) ENE (c) EXE

3.3. Effect of O_2/fuel ratio

The effect of O_2/F ratio on syngas composition for untreated and IL-treated coal samples is illustrated in **Figure 6**. Temperature (900°C) and S/F ratio (2.85) were kept constant. As the amount of O_2 increases, carbon conversion also increases. However, an excess amount of O_2 results in incomplete combustion of fuel, thereby reducing the quantity of syngas. Therefore, O_2/F ratio was varied between 0.1 and 0.6. It was observed that CO and H_2 decreased with an increase in O_2/F, in contrasting fashion (H_2 decreasing more rapidly than CO), whereas CO_2 and CH_4 increased. As O_2 supply is increased, carbon and hydrogen conversion reactions are facilitated, resulting in a decrease in CO and H_2 and a rise in CO_2 and CH_4. Concerning CO, contrasting profiles were observed for IL-treated samples, with RC_3 creating a wide gap as compared to untreated coal, while RC_1, RC_2, and RC_4 were sandwiched between them.

As expected, CO_2 concentration increases in all the samples with the rise in the O_2/F ratio. The amount of CO_2 production was found to be directly proportional to the O_2 concentration in the samples. This might be the reason for RC_3 to register the lowest values throughout the flow range, with the margin widening as the ratio increased. All the ILs decreased CO_2 production, which is a positive sign from the environmental point of view. As regards H_2, all the samples experienced a sharp decrease. However, in the case of [P_{66614}] [Cl] treated coal, the decline was somewhat less pronounced. Except [P_{66614}] [Cl], all other samples showed an increase in methane production with the O_2/F ratio. This is caused by their

elemental composition. H_2/CO ratio decreased sharply with O_2/F for all the samples except [P_{66614}] [Cl], which remained constant. Due to higher carbon content, the WGS reaction is dominant in the gasification of [P_{66614}] [Cl] treated sample, which does not allow H_2 to dip sharply, thereby resulting in a stable H_2/CO ratio.

LHV of all the samples suffered a decrease with the rise in O_2 supply. This is expected since the increase in the O_2/F ratio reduces CO and H_2 in the syngas. Comparatively, [P_{66614}] [Cl] treated coal gave the highest LHV values throughout, due to high H_2 content.

Figure 7 represents the effect of the O_2/F ratio on CGE, ENE, and EXE at constant temperature (900°C) and S/F ratio (2.85). Like temperature, for the O_2/F ratio, CGE and EE reported almost identical values for all the studied samples. A sharp decline was observed for both CGE and EE with the O_2/F ratio. This happens due to a decrease in the HHV of syngas caused by a reduction in the concentration of H_2 and CO. Highest values were recorded by [P_{66614}] [Cl] as a result of higher HHV of syngas. In terms of EXE, untreated coal showed higher values in the beginning due to high β values. However, as O_2 supply increases, EXE dips sharply because the slow rise in the exergy of the syngas is not enough to offset the increase in the exergy of steam. On the contrary, in the case of [P_{66614}] [Cl], the high chemical exergy of the syngas keeps the decrease in check throughout the rise in the O_2 supply.

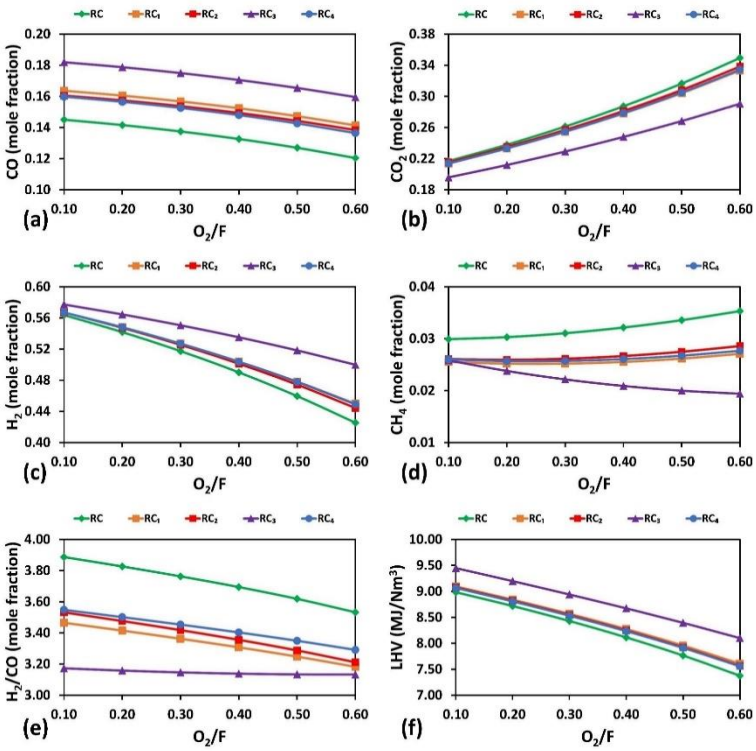

Figure 6: Effect of O_2/F ratio at T=900°C and S/F=2.85 on syngas composition (a) CO (b) CO_2 (c) H_2 (d) CH_4 (e) H_2/CO

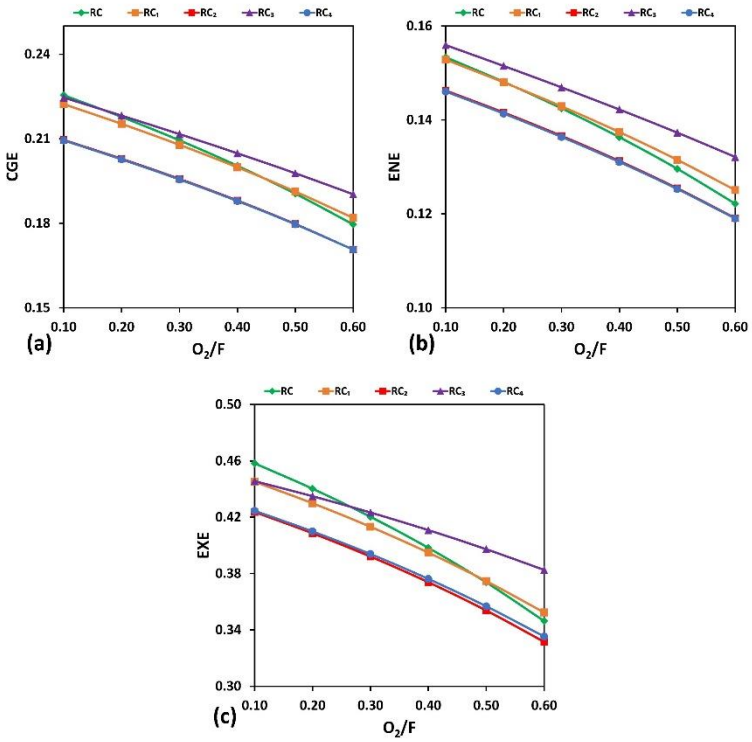

Figure 7: Effect of O_2/F ratio at T=900°C and S/F=2.85 on (a) CGE (b) ENE (c) EXE

3.4. Effect of steam/fuel ratio

Figure 8 displays the effect of the S/F ratio by varying it between 2-4 on syngas composition at a constant temperature (900°C) and O_2/F ratio (0.6). Steam increases the concentration of H_2 and CO in the syngas owing to the WGS reaction. However, the CO shift reaction (**Table 2**) predicts the conversion of CO to CO_2. The results obtained from the model agree with these predictions, i.e., H_2 and CO_2 increase while CO decreases. For CO, the slope for all the samples is almost the same, except [P_{66614}] [Cl], which gives a somewhat sharper slope. The reason for this is the higher concentration of carbon and a lower concentration of O_2 in these samples. Therefore, higher CO was obtained at a low S/F ratio and reduced sharply as the steam supply increased due to the dominance of the CO shift reaction. CO_2 concentration was directly correlated with the quantity of O_2 in the samples. The concentration of H_2 is correlated with the quantity of carbon in the samples due to the dependency of CO and H_2 on the WGS process, where carbon serves as a catalyst. The concentration of CH_4 remained rather stable despite an increase in the S/F ratio.

The syngas composition results predicted by the model on varying O_2/F ratios are in agreement with the earlier reports [34].

The H_2/CO ratio increases linearly for untreated and IL-treated samples. The sharpest rise was observed in the case of [P_{66614}] [Cl], which can be predicted from H_2 and CO content. Untreated coal recorded

the highest ratios due to low CO content. For LHV, [P_{66614}] [Cl] treated coal gave the highest values throughout, while untreated coal gave the lowest values.

Figure 9 represents the effect of the S/F ratio on CGE, EE, and EXE at constant temperature (900°C) and O_2/F ratio (0.6). CGE decreased slightly with the rise in the S/F ratio, with [P_{66614}] [Cl] reporting the highest decline. This is due to the sharp reduction in methane concentration in the case of [P_{66614}] [Cl]. The same trend and order were observed for EE. In terms of EXE, [P_{66614}] [Cl] reported by far the highest values reaching a peak of 38%.

The same trend and order were observed for ENE. In terms of EXE, [P_{66614}] [Cl] reported by far the highest values reaching a peak of 35%.

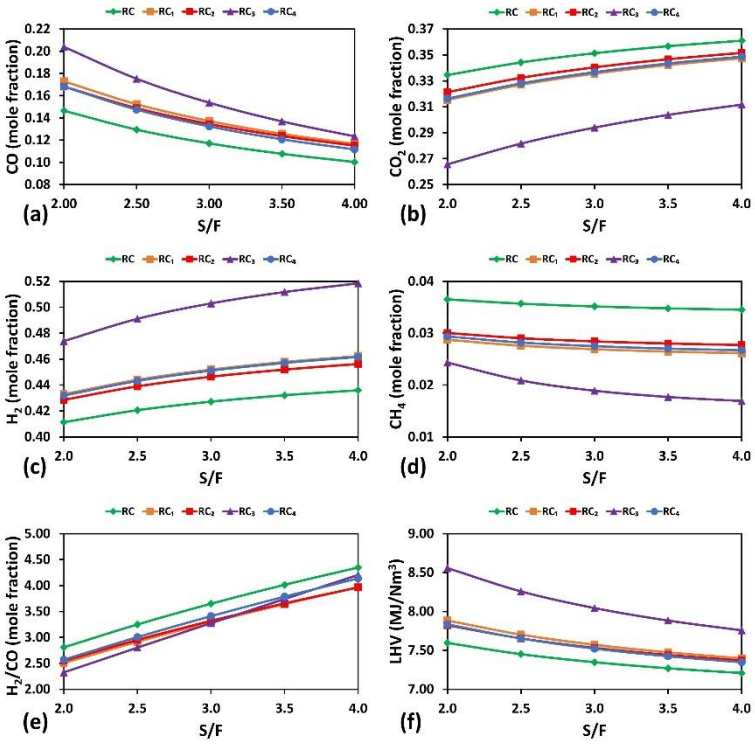

Figure 8: Effect of S/F ratio at T=900°C and O_2/F=0.6 on syngas composition (a) CO (b) CO_2 (c) H_2 (d) CH_4 (e) H_2/CO (f) LHV

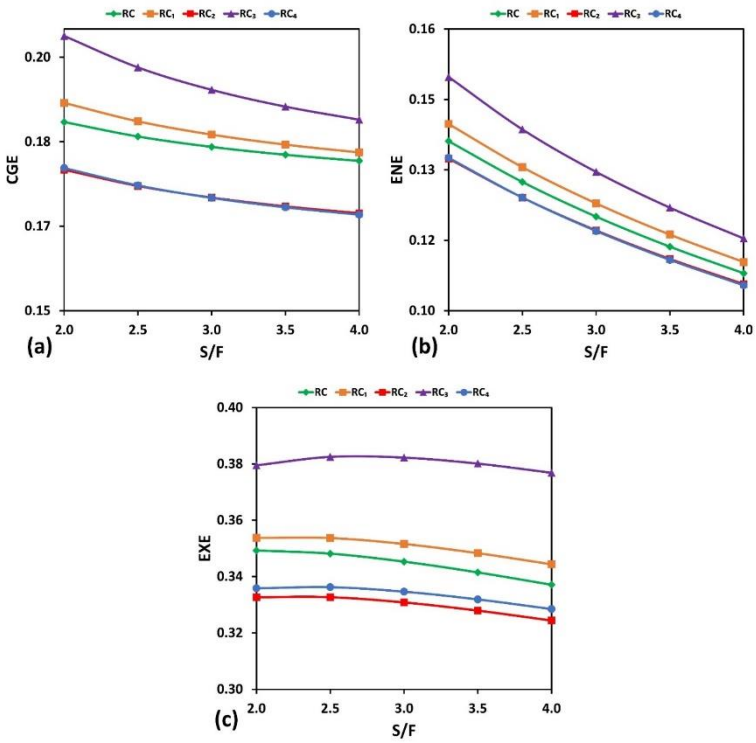

Figure 9: Effect of S/F ratio at T=900°C and O_2/F=0.6 on (a) CGE (b) ENE (c) EXE

4. CONCLUSIONS

The effect of IL pretreatment on coal gasification was investigated through an equilibrium-based simulation model in Aspen Plus®. Four ILs based on different cations combined with chloride anion were used for pretreating low-rank Pakistani coal. An Aspen Plus® equilibrium-based steam-O_2 gasification model was used to do comparative and sensitivity analysis of untreated and IL-pretreated coal samples. Comparative analysis of gasification performance was made at the standard model conditions of T=900°C, O_2/F=0.6, and S/F=2.85. IL treatment increased CO and H_2 and decreased CO_2 and CH_4, which signifies the eco-friendly characteristics of ILs. [P_{66614}] [Cl] had the greatest effect, nearly halving the CH_4 amount. This may be due to the assimilation of [P_{66614}] [Cl] in coal, leading to a substantial change in the elemental makeup. [P_{66614}] [Cl] upgraded the low-rank coal, increasing the carbon content from 57.77 to 82.75%, which equals a 43% increase. This leads to an H_2-rich syngas, confirmed by the simulation results. IL pretreatment resulted in the production of H_2-rich syngas by WGS and reverse methanation reactions. The reason could be the increase in the carbon content of coal brought about by IL pretreatment. Additionally, the ILs improved the LHV of coal, a crucial metric for determining its efficiency. It can be concluded that relatively unknown and low-cost ammonium and phosphonium-based ILs could be eco-friendly and promising pretreatment solvents for the coal gasification process. Commercialization of thermochemical conversion of IL-pretreated low-grade coal still faces a lot of obstacles and needs further extensive research. Identification of non-toxic and low-cost ILs is necessary for the upscaling of the process from lab to pilot scale and eventually to commercial scale. Future research might benefit from an economic comparison of untreated and treated thermochemical conversion processes for IL. Furthermore, the potential impact of underlying mineral behavior in coal after IL pretreatment on the overall outcomes warrants further investigation in the future.

5. DECLARATION

The authors declare no competing financial interest.

6. ACKNOWLEDGMENT

The authors express their gratitude to the management of the Coal Research Center (CRC) in the NFC Institute of Engineering & Technology for supporting this research.

7. REFERENCES

[1] Bhandary, R. R. and Gallagher, K. S., What drives Pakistan's coal-fired power plant construction boom? Understanding the China-Pakistan Economic Corridor's energy portfolio, *World Dev. Perspect.*, 25, 100396, (2022).

[2] Nisar, J., Awan, I. A., Iqbal, M., Abbas, M., and ---, S., Pyrolysis–Gas Chromatography of

Lakhra Coal: Effect of Temperature and Inorganic Matter on the Product Distribution, *Iran. J. Chem. Chem. Eng.*, 38(6):, 297–305, (2019).

[3] Ahmad, T., Awan, I. A., Nisar, J., and Ahmad, I., Influence of inherent minerals and pyrolysis temperature on the yield of pyrolysates of some Pakistani coals, *Energy Convers. Manag.*, 50(5):, 1163–1171, (2009).

[4] Nisar, J., Ullah, N., Awan, I. A., Khan, K., and Ahamd, I., Characterization of the Products Obtained in Coal Pyrolysis: A Case study of Some Pakistani Coals, *Iran. J. Chem. Chem. Eng.*, 30(3):, 53–56, (2011).

[5] Saeed, S. and Saleem, M., Novel Pretreatment Methods to Improve Enzymatic Saccharification of Sugarcane Bagasse: A Report, *Iran. J. Chem. Chem. Eng.*, 37(5):, 225–234, (2018).

[6] Pin, T. C., Nakasu, P. Y. S., Mattedi, S., Rabelo, S. C., and Costa, A. C., Screening of protic ionic liquids for sugarcane bagasse pretreatment, *Fuel*, 235, 1506–1514, (2019).

[7] Khan, S. S., Saeed, S., and Riaz, M., Reactivity, kinetic, and thermodynamic analysis of ionic liquid assisted thermal degradation of spent coffee ground, *Iran. J. Chem. Chem. Eng.*, (2022).

[8] Kazmi, B., Haider, J., Qyyum, M. A., Saeed, S., Kazmi, M. R., and Lee, M., Heating load depreciation in the solvent-regeneration step of absorption-based acid gas removal using an ionic liquid with an imidazolium-based cation, *Int. J. Greenh. Gas Control*, 87, 89–99, (2019).

[9] Haider, J. *et al.*, Simultaneous capture of acid gases from natural gas adopting ionic liquids: Challenges, recent developments, and prospects, *Renew. Sustain. Energy Rev.*, 123, 109771, (2020).

[10] Painter, P., Pulati, N., Cetiner, R., Sobkowiak, M., Mitchell, G., and Mathews, J., Dissolution and Dispersion of Coal in Ionic Liquids, *Energy & Fuels*, 24(3):, 1848–1853, (2010).

[11] Liang, P. *et al.*, Effects of ionic liquid pretreatment on pyrolysis characteristics of a high-sulfur bituminous coal, *Fuel*, 258, 116134, (2019).

[12] Saeed, S. *et al.*, Pyrolysis of ionic liquid pretreated lignite: Effect of 1-butyl-3-methylimidazolium methyl sulfate pretreatment on kinetic and thermodynamic parameters of lignite, *Energy Sources, Part A Recover. Util. Environ. Eff.*, 1–17, (2021).

[13] Saeed, S., Saleem, M., and Durrani, A., Thermal performance analysis of sugarcane bagasse pretreated by ionic liquids, *J. Mol. Liq.*, 312, 113424, (2020).

[14] Lei, Z. *et al.*, Pyrolysis of lignite following low temperature ionic liquid pretreatment, *Fuel*, 166, 124–129, (2016).

[15] Xu, Y., Liu, Y., Bu, Y., Chen, M., and Wang, L., Review on the ionic liquids affecting the desulfurization of coal by chemical agents, *J. Clean. Prod.*, 284, 124788, (2021).

[16] Bai, Z., Wang, C., and Deng, J., Analysis of thermodynamic characteristics of imidazolium-based ionic liquid on coal, *J. Therm. Anal. Calorim.*, 140(4):, 1957–1965, (2020).

[17] Yoon, S., Deng, L., Namkung, H., Fan, S., Kang, T.-J., and Kim, H.-T., Coal structure change by ionic liquid pretreatment for enhancement of fixed-bed gasification with steam and CO2, *Korean J. Chem. Eng.*, 35(2):, 445–455, (2018).

[18] S, G. and P.K.., D., Optimization and Prediction of Reaction Parameters of Plastic Pyrolysis oil Production Using Taguchi Method, *Iran. J. Chem. Chem. Eng.*, 39(2):, 91–103, (2020).

[19] Saeed, S., Saleem, M., and Durrani, A. K., Thermal performance analysis of low-grade coal pretreated by ionic liquids possessing imidazolium, ammonium and phosphonium cations, *Fuel*, 271, 117655, (2020).

[20] Kazmi, S. M. B., Awan, Z. H., and Hashmi, S., Simulation study of ionic liquid utilization for desulfurization of model gasoline, *Iran. J. Chem. Chem. Eng.*, 38(4):, 209–221, (2019).

[21] Gheewala, S., Abid, L., Khan, S. S., Ghani, U., and Mahmood, A., Sensitivity analysis of coal and bagasse co-firing in an Integrated Gasification Combined Cycle Power Plant, *Iran. J. Chem. Chem. Eng.*, (2022).

[22] Ajorloo, M., Ghodrat, M., Scott, J., and Strezov, V., Recent advances in thermodynamic analysis of biomass gasification: A review on numerical modelling and simulation, *J. Energy Inst.*, 102, 395–419, (2022).

[23] Nikoo, M. B. and Mahinpey, N., Simulation of biomass gasification in fluidized bed reactor using ASPEN PLUS, *Biomass and Bioenergy*, 32(12):, 1245–1254, (2008).

[24] Wen, C. Y. and Chaung, T. Z., Entrainment Coal Gasification Modeling, *Ind. Eng. Chem. Process Des. Dev.*, 18(4):, 684–695, (1979).

[25] Suuberg, E. M., Peters, W. A., and Howard, J. B., Product Composition and Kinetics of Lignite Pyrolysis, *Ind. Eng. Chem. Process Des. Dev.*, 17(1):, 37–46, (1978).

[26] Okumura, Y. and Okazaki, K., Prediction of pyrolysis products and yields from brown to semi-anthracite coals by using elemental composition, *Nihon Enerugi Gakkaishi/Journal Japan Inst. Energy*, 89(4):, 364–372, (2010).

[27] Rupesh, S., Muraleedharan, C., and Arun, P., ASPEN plus modelling of air–steam gasification of biomass with sorbent enabled CO2 capture, *Resour. Technol.*, 2(2):, 94–103, (2016).

[28] Ramzan, N., Ashraf, A., Naveed, S., and Malik, A., Simulation of hybrid biomass gasification using Aspen plus: A comparative performance analysis for food, municipal solid and poultry waste, *Biomass and Bioenergy*, 35(9):, 3962–3969, (2011).

[29] Rupesh, S., Muraleedharan, C., and Arun, P., Energy and exergy analysis of syngas production from different biomasses through air-steam gasification, *Front. Energy*, 1–13, (2016).

[30] Karimipour, S., Gerspacher, R., Gupta, R., and Spiteri, R. J., Study of factors affecting syngas quality and their interactions in fluidized bed gasification of lignite coal, *Fuel*, 103, 308–320, (2013).

[31] Hussain, M., Tufa, L. D., Yusup, S., and Zabiri, H., A kinetic-based simulation model of palm kernel shell steam gasification in a circulating fluidized bed using Aspen Plus®: A case study, *Biofuels*, 9(5):, 635–646, (2018).

[32] Saeed, S., Saleem, M., and Durrani, A. K., Thermal performance analysis of low-grade coal pretreated by ionic liquids possessing imidazolium, ammonium and phosphonium cations, *Fuel*, 271, 117655, (2020).

[33] Tauqir, W., Zubair, M., and Nazir, H., Parametric analysis of a steady state equilibrium-based biomass gasification model for syngas and biochar production and heat generation, *Energy Convers. Manag.*, 199, 111954, (2019).

[34] Eri, Q., Wu, W., and Zhao, X., Numerical Investigation of the Air-Steam Biomass Gasification Process Based on Thermodynamic Equilibrium Model, *Energies*, 10(12):, 2163, (2017).